ESCUELA TÉCNICA SUPERIOR DE INGENIEROS
INDUSTRIALES Y DE TELECOMUNICACIÓN

UNIVERSIDAD DE CANTABRIA

Trabajo Fin de Grado

UN MODELO CINÉTICO PRIMARIO PARA LA OXIDACIÓN DE FURFURAL CON PERÓXIDO DE HIDRÓGENO
(A PRIMARY KINETIC MODEL FOR FURFURAL OXIDATION WITH HYDROGEN PEROXIDE)

Para acceder al Título de

Graduada en Ingeniería Química

Autora: Yiran Chen

A PRIMARY KINETIC MODEL FOR FURFURAL OXIDATION WITH HYDROGEN PEROXIDE

Master's Thesis

Yiran Chen

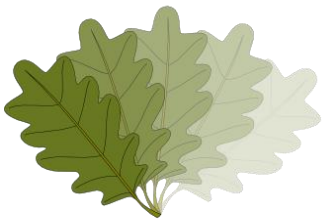

Johan Gadolin
Process Chemistry Centre

Laboratory of Industrial Chemistry and Reaction Engineering
Faculty of Science and Engineering /Chemical Engineering
Åbo Akademi University
Turku/Åbo 2016

Abstract

The present work is focused on preliminary modelling of furfural oxidation to organic acids over a heterogeneous Smopex-101.

The objective was fitting in of the experimental data with a possible reaction mechanism by using modelling and optimization software. Before the model was created, a mass balance for each reactant was calculated, which included: determination of the residence time distribution and the volume measurement for the system, the gas-liquid equilibrium and solubility of carbon dioxide during the reaction.

Once the mass balance was obtained, it was applied to a supposed simplified reaction mechanism. Therefore, two models based on it were implemented and analyzed. A hypothesis various routes for generation of an intermediate formic acid, was verified.

Further studies about consumption of hydrogen peroxide are required for a more precise reaction mechanism.

Keywords: Residence time distribution, formic acid, succinic acid, kinetic modelling.

Resumen

El presente trabajo es un estudio primario de la oxidación de furfural a ácidos orgánicos con un catalizador heterogéneo (Smopex-101).

El objetivo principal fue ajustar los datos experimentales con un mecanismo hipotético simplificado de reacción utilizando un modelo cinético creado con el programa Modest. Antes de realizar el modelo, el balance de materia de cada componente fue calculado, tomando en cuenta los siguientes aspectos: la determinación de la distribución del tiempo de residencia y la medición de volumen del sistema, el equilibrio entre gas-líquido y la solubilidad del dióxido de carbono durante la reacción.

Después de obtener del balance de materia, éste fue aplicado al mecanismo de reacción hipotético y simplificado. Más tarde, dos modelos basados en este mecanismo fueron ejecutados y analizados. Fue verificada, la hipótesis de la existencia de una especie intermediaria, que pueda ser generada simultánea y equimolarmente con el ácido fórmico durante la reacción. Además de esta reacción, también existen otras fuentes de formación del mismo acido que requieren más estudios para la identificación.

Finalmente, futuros estudios sobre el consumo del peróxido de hidrogeno son necesarios, para obtener un mecanismo de reacción más preciso.

Keywords: Distribución de tiempo de residencia, ácido fórmico, ácido succínico, modelo cinético.

Acknowledgment

First of all I want to express my gratitude to Professor Tapio Salmi and Dmitry Yu Murzin for giving me the opportunity to work with this project in such an amazing working atmosphere at the Department of Chemical Engineering. I am really grateful that Farhan Saleem, my supervisor, who has been guiding me and helping me with all the problems during this work. Moreover I want to thank Kari Eränen and Johan Wärnå, who helped me during the experimental work and kinetic modelling.

To Karen, Marina, Inés and David, my dearest friends, for all the supports and encouragement far away from Spain. I am grateful to my friends for sharing nice experience and moments in my exchange semester in Åbo: Shuyana, Minh, Gioele, Alice, Virginia, Hanyan Hua, Adriana and Andrea.

感谢我们的天父以及我的家人，谢谢父亲给我的支持。致我的母亲和妹妹，感谢你们一直以来的陪伴和付出，对我不间断的信任和鼓励。我会继续努力，变成一个优秀的人，不让你们失望的。

Para acabar, gracias, a Alejandro.

Åbo, Finland, May 2016

Table of contents

Nomenclature

E_a	Reaction activation energy
a_0	Mass transfer area-to-volume
k_{Li}	Mass transfer coefficient
A	Interfacial area
H	Henry's law coefficient
H	Henry's law constant
I	Intensity (in mass spectroscopy)
I	Intermediate (in reaction mechanism)
K	Liquid-gas equilibrium constant
N	Interfacial transfer coefficient
P	Pressure
R	Ideal gas constant
T	Temperature
V	Volume
c	Concentration
k	Reaction rate constant
m	Mass
n	Molar number
r	Reaction rate
t	Time
$vol\%$	Volume percentage
x	Molar fraction in liquid phase
y	Molar fraction in gas phase
$wt\%$	Weight percentage

Abbreviations	**Name**
CO_2	Carbon dioxide in gas phase
F	Furfural
FoA	Formic acid
FumA	Fumaric acid
FurA	Furoic acid
Hf	2 (5H) furanone
HP	Hydrogen peroxide
Me	Maleic acid
Mi	Malic acid
Mo	Malonic acid
SA	Succinic acid
W	Water
cat	Catalyst

Subscripts and superscripts	Name
-	Direction from product to reactant
--	Mean value
+	Direction from reactant to product
$*$	Interfacial value (liquid-gas film)
0	Initial amount
cat	Catalyst
G	Gas phase
i	Component index
in	Inlet
L	Liquid phase
mean	Mean value
out	Outlet
R	Reactor (excluding the dead volume)
t	Total amount
eq	Equilibrium value

Greek symbols	Name
$\hat{\phi}_i$	fugacity coefficient for component i
α	$\frac{V_{0L}}{V_G}$
θ	Dimensionless time
ν	Volume flowrate of gas
ρ	Density
τ	Reactor holding time
δ	Liquid-gas film thickness

1 Introduction

Furfural is produced with the only commercial route, the acid-catalyzed digestion of hemicellulose-rich agricultural waste. Furfural undergoes reactions typical for aldehydes like acetalization, acylation, aldol and Knoevenagel condensations, reduction to alcohols, reductive amination to amines, decarbonylation, oxidation to carboxylic acids, and Grignard reactions. The aldehyde group of furfural easily undergoes catalytic oxidation to furoic acid in the presence of oxygen, air, or hydrogen peroxide [1].

Hydrogen peroxide occurs naturally in the environment. It is strongly related to the oxygen-containing atmosphere of our planet and adaption of nature to oxygen. Therefore, it is a really environmentally-friendly oxidant [2].

During furfural oxidation reaction over catalyst Smopex-101, there are many carboxylic products, such as: furoic, maleic, malic, malonic, succinic, formic acids and 2-(5H) furanone. The most interesting chemical among them is succinic acid, a dicarboxylic acid that occurs naturally in plant and animal tissues. It is applied in a number of industries including polymers (clothing fibres), food, surfactants and detergents, flavours and fragrances [3]. Succinic acid was named as one of the "*Top Value Added Chemicals From Biomass*" by the U.S. Department of Energy [4] and there are companies who are producing bio-based succinic acid [5], [6].

Furthermore, the reaction is quite important from the industrial viewpoint, even if theoretical knowledge about this reaction is quite limited. Thus, a simplified reaction mechanism was advanced in this work. Kinetic modelling was applied for verification of the mechanism. In the present thesis an attempt is made to study the reaction kinetics, gas-liquid phase equilibrium and the residence time distribution for the gas phase in the reactor. After the analysis of the experimental data, simplified reaction mechanisms were suggested and applied for kinetic modelling.

2 Aims and objectives

The objectives of the present thesis can be stated as follows:

- Determination of the residence time distribution of the gas in the system.
- Study of the gas-liquid equilibrium and its application to the mass balance.
- Proposal of a tentative of reaction mechanism.
- By using kinetic modelling, the proposed reaction mechanism was verified.

3 Theoretical section

3.1 Residence time distribution (RTD)

The hydrodynamic behaviour of a reactor is not always ideal, since there could be possible fluid short cut or dead volume in the reactor. Therefore, the concept of RTD is really helpful to resolve this problem, which is essentially a statistical approach for description of the fluid flow. When an element of the fluid enters to the reactor, it is considered until it leaves the reactor. *Residence-time distribution* is a curve which presents probability of a particle leaving the reactor after a certain residence time [7].

The RTD of a reactor is usually presented in terms of the *frequency distribution*, the E curve (Figure 3-1).

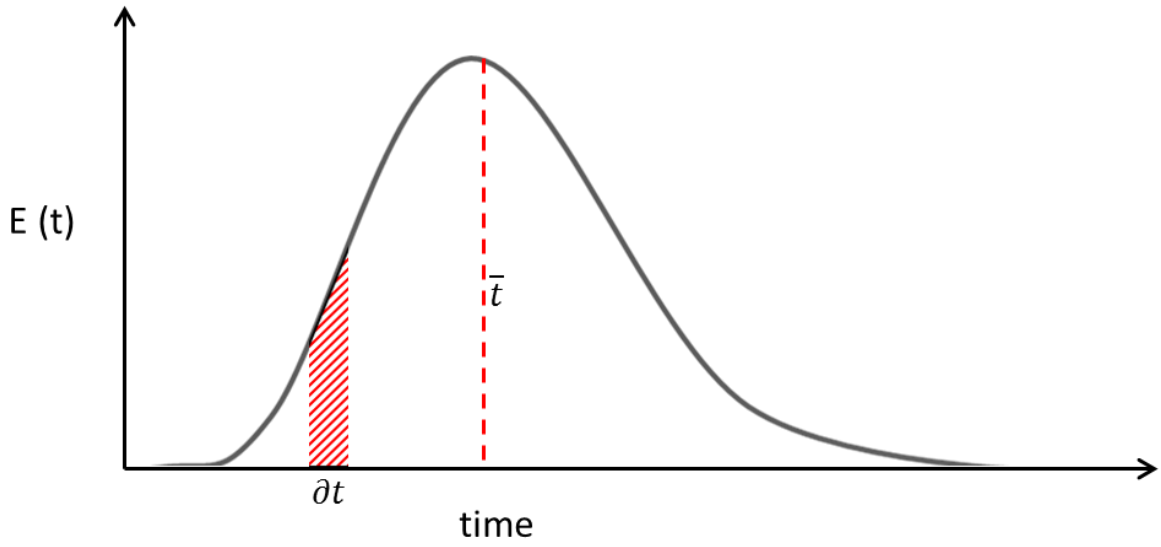

Figure 3-1 The RTD given by the E(t) diagram, the shaded area E(t) ∂t represents the probability of a fluid element having a residence time between t and t+∂t.

The area under the curve is equal to 1, since E(t) is the normalized response, which means:

$$\int_0^\infty E(t)\,\partial \mathrm{t} = 1 \qquad (3\text{-}1)$$

The E diagram is often also presented by the dimensionless time θ by plotting E(θ) versus θ. The definition of θ is:

$$\theta = \frac{t}{\tau} \qquad (3\text{-}2)$$

where τ is the holding time, being related to the accessible volume reactor:

$$\tau = \frac{V}{\nu} \qquad (3\text{-}3)$$

In equation above, V is the accessible reactor volume and ν is the fluid volumetric flow rate.

Normally the holding time is equal to the average residence time, but it can also differ from it. For example, if there is adsorption, the average residence time is longer than the holding time:

$$\tau < \bar{t} \qquad (3\text{-}4)$$

For the carried out in the current work, the adsorption phenomena are assumed negligible, since both the catalyst and the reactant are fed in the solid and gas phases, and then the average residence time and the holding time for the gas phase are equal:

$$\tau = \bar{t} \qquad (3\text{-}5)$$

In addition to E curves, C curves are usually used and having the same shape.

3.1.1 Tracer experiments – the pulse method

There are three major categories of experimental methods for determining RTDs [8]:

- The pulse method.
- A stepwise introduction of the tracer.
- A periodically changing supply of the tracer.

The pulse method is the one selected in the current work, since in the studied system there was no tracer gas supplier channel and it was considered to be more complicated to carry out other methods for RTD. It consists in injecting a certain amount of tracer to the system in a very short time interval, forming a pulse. A normal pulse experiment in a continuous stirred-tank reactor can give a response similar to presented in Figure 3-2:

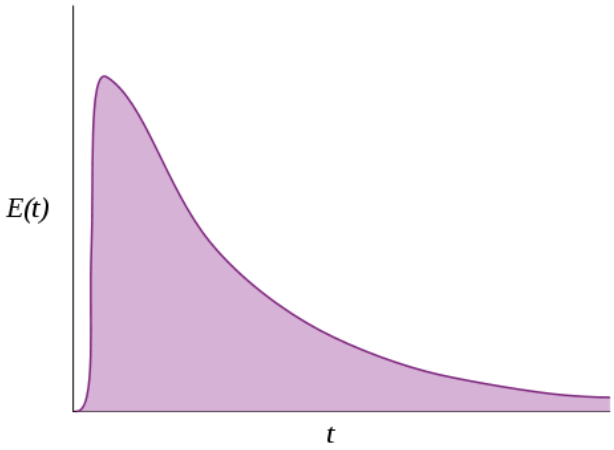

Figure 3-2 E curve of a pulse experiment response.

The tracer experiment is a really helpful tool for knowing about distribution of the fluid in a reactor, especially when a system contains lots of accessories or is a combination of reactors. In Figure 3-3, diagnostic of the reactor fluid behaviour are presented, which was used for the tracer response curves analysis.

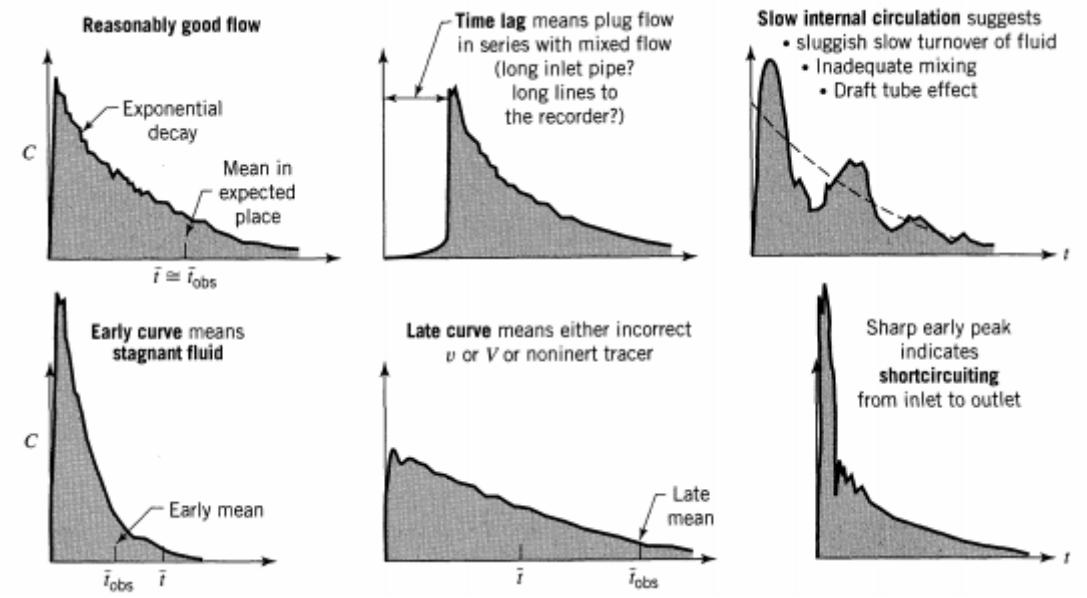

Figure 3-3 Behaviour of mixed flow reactors. [9]

3.1.2 Mass spectroscopy

In the present thesis, the liquid phase was in batch mode, while semi-batch was considered for the gas phase. Thus a residence time distribution should be determined for the gas phase. As it is a semi-batch operation, the outlet variable can be measured on-line, which means that the instrument should be installed at the outlet of the reactor [8], as presented in Figure 3-4.

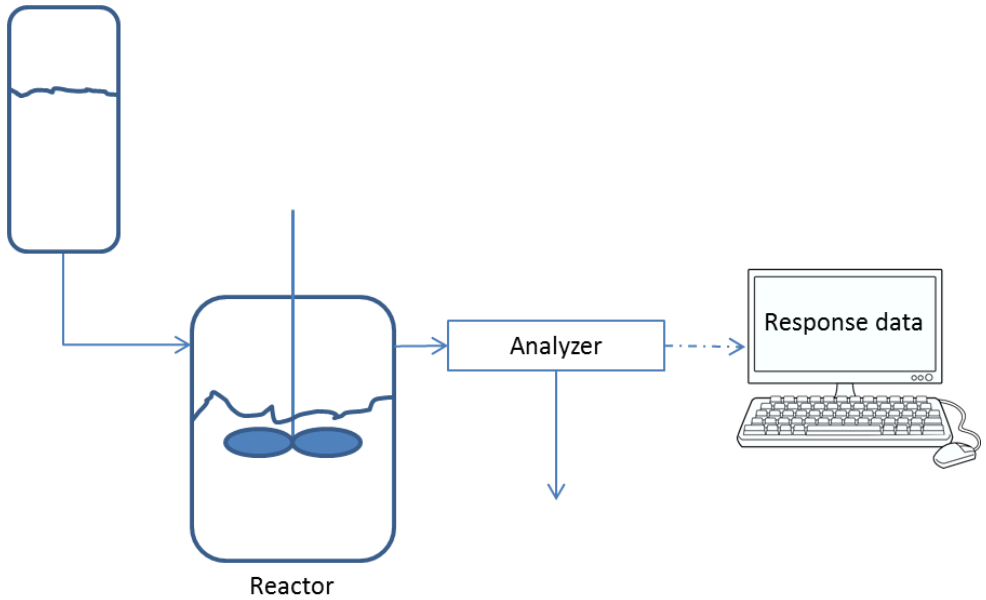

Figure 3-4 Apparatus for the experimental determination of RTD in a continuous reactor.

There are many analytical methods for conducting tracer experiments in continuous reactors (Table 3-1). In the current work only mass spectroscopy is suitable, since the tracer experiment was applied for the gas phase.

Table 3-1 Common Analytical Methods for Tracer Experiments in Continuous Operations [8]

Method	Measuring Principle
Conductometry	Electrical conductivity
Photometry	Light absorbance (visible or UV light)
Mass spectroscopy	Different mass numbers of components
Paramagnetic analysis	Paramagnetic properties of compounds
Radioactivity	Radioactive radiation

3.2 Reaction kinetics

3.2.1 Reaction kinetics of catalytic reactions

The reaction rate equation of a catalytic reaction is related to the catalyst concentration and the rate constant. Considering a following reaction:

$$A + B + catalyst \leftrightharpoons C + catalyst$$

The rates in the forward and reverse directions are:

$$r_+ = k_+ c_A c_B c_{cat} \qquad (3\text{-}6)$$

$$r_- = k_- c_c c_{cat} \qquad (3\text{-}7)$$

At equilibrium:

$$k_{eq} = \frac{k_+}{k_-} \qquad (3\text{-}8)$$

The rate constants are independent on concentrations, while the units depend on the reaction order. [10]

3.2.2 Quasi-equilibrium steady state assumption

The equilibrium reaction rate is not usually studied, instead of it, the reaction rates away from equilibrium are analysed [11]. In furfural transformations, several compounds are formed. Quasi-equilibrium steady-state assumption was applied for intermediates in the hypothetical reaction mechanism in the present thesis (section 6.4.2).

The principles of quasi-equilibrium can be explained for the reaction [8]:

$$A \leftrightharpoons R \leftrightharpoons S$$

where R is a quickly reacting intermediate.

If the first reaction has a much rapid rate compared with others ($r_1 \gg r_2$) as shown in Figure 3-5, the net generation rate of intermediate R is practically zero ($r_R = 0$), which means:

$$r_R = r_{R,formation} - r_{R,consumption} = 0 \qquad (3\text{-}9)$$

By substituting expressions of each reaction:

$$r_R = r_{1+} - r_{1-} - r_{2+} + r_{2-} = 0 \qquad (3\text{-}10)$$

Thus, **¡Error! No se encuentra el origen de la referencia.** can be applied for every intermediate species

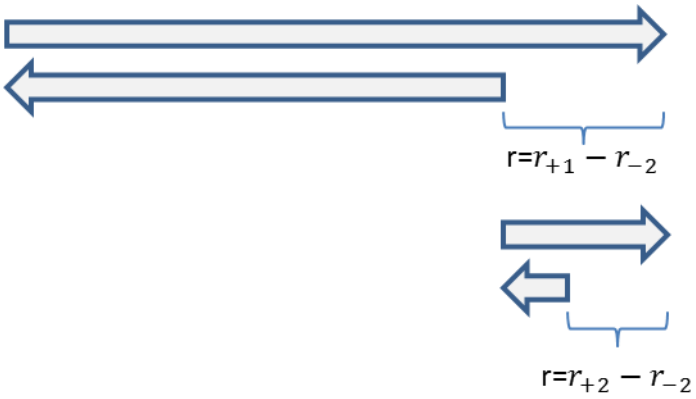

Figure 3-5 Quasi-equilibrium hypothesis description.

3.3 Reaction mass balance

3.3.1 Batch and semi-batch reactors

A combination of reactors is involved in the present system: batch reactor for the liquid phase and semi-batch mode is considered for the gas phase.

Batch reactor is the one in which reactants are charged at beginning of the operation, and products will not be discharged until the end of the operation. Normally, the reactor is agitated for efficient mixing of reactants therefore the mass transfer resistances in the system can be neglected and uniform conditions can be attained throughout the vessel [12].

Semi-batch mode is similar to the batch reactor with the difference that, the reactants are added or products are taken out during the operation. This mode of operation is used when certain selectivity or the reaction rate is desirable. It is also used to modify the reaction conditions inside the reactor, such as temperature or pressure [12].

3.3.2 Liquid-gas equilibrium

The transport phenomena have an important role in the mass balance when the reactor is heterogeneous. As some gases are soluble in the liquid phase, liquid-gas equilibrium is usually studied. In the present thesis, there are two main components in the gas phase, oxygen and carbon dioxide. Carbon dioxide's equilibrium was studied since oxygen was assumed that is negligible (explained in the section 5.1.1). Henry's law, two-film theory and the Fick's law were used for the equilibrium calculation.

First, the Henry's law was used to obtain CO_2 concentration in the liquid phase (see section 5.1). Then the concentration was applied with two-film theory and Fick's law for the mass transfer phenomena in the mass balance in section 3.3.3.

Normally, Henry's law is applied for infinitely dilute solutions at low pressures, having the following form:

$$P_i = x_i H_{i,L} \qquad (3\text{-}11)$$

where i is the gaseous component and L refers to the solvent.

The Henry's law constant depends only on temperature and can be determined from the solubility equilibria with the solubility data. Solubility data have been mainly defined as the ratio of the amount of gas dissolved at the partial pressure $P_i = 1$ to the amount of solvent.

For gases there is no temperature limit for applying this law. Henry's law constant has the same dimensions as the vapour pressure and is numerically equal to it in ideal solutions [13]. In this thesis an ideal solution of carbon dioxide and water was assumed.

In addition, a constant K, is frequently applied in the design of industrial processes to study the mass transfer effects, as it can be used to calculate the solubility equilibria of hydrocarbons in petrochemicals. Therefore, it was also used in this thesis. K_i has the following definition, according to the literature [13]:

$$K_i = \frac{y_2}{x_2} \qquad (3\text{-}12)$$

The K values do not depend on the solvent composition, but only on temperature and total pressure. By relating it with the Henry's law, the K value can be written as:

$$H_i = K_i P \qquad (3\text{-}13)$$

There are many theories and methods for the calculation of molar fluxes in heterogeneous systems. A particularly simple but useful model for steady-state transfer between two phases is the two-film theory (Figure 3-6).

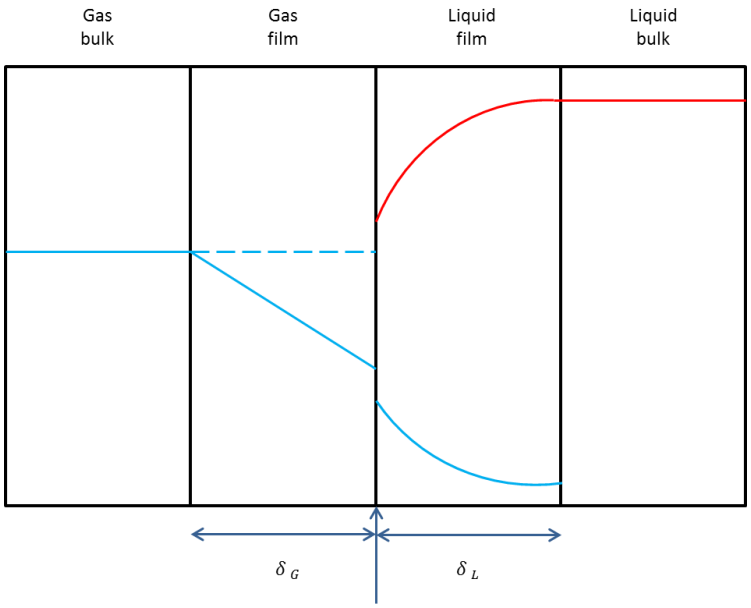

Figure 3-6 Diffusion and reaction in gas and liquid films, where the red line presents the product and the blue line the reactant [8].

If the Fick's law is valid for both films it holds [8]:

$$N_i = k_{Li}(c_{Li} - c_{Li}^*) \qquad (3\text{-}14)$$

where N_i is the interfacial transfer coefficient, c_{Li} is the concentration of the component in the liquid and c_{Li}^* is the concentration at the liquid-gas interface. The following expression of the mass transfer coefficient can be obtained [8]:

$$k_{Li} = \frac{D_i}{\delta} \qquad (3\text{-}15)$$

where, k_i is the mass transfer coefficient, D_i is the diffusivity and δ the film thickness.

This theory was used also to derive the expression of the equilibrium constant between gas and liquid phases (K_i), which is described in the section 5.1.1.

3.3.3 Mass balance for gas and liquid phases

The general mass balance for all components is written as follow:

[In] + [Generated] = [Out] + [Accumulated]

Therefore for an arbitrary component (i) in the liquid phase, the mass balance is written in a quantitative form as follows:

$$\dot{n}_{Li,in} + r_i V_{0L} \frac{m_{cat}}{V_{Li}} = \dot{n}_{Li,out} + N_i A + \frac{dn_{Li}}{dt} \qquad (3\text{-}16)$$

In this case, the liquid phase is considered in a batch mode, thus there are no in and out flows. According to the Fick's law (equation (**3**-**14**)), the only outflow is caused by the interfacial transfer (N_i).

Moreover the number of moles is equal to:

$$n_{Li} = C_{Li} V_L \qquad (3\text{-}17)$$

As the liquid volume almost does not vary during experiments, it is assumed to be constant. Therefore the mass balance becomes:

$$r_i V_{0L} \frac{m_{cat}}{V_L} = A k_{Li} (c_{Li} - c_{Li}^*) + V_{0L} \frac{dC_{Li}}{dt} \qquad (3\text{-}18)$$

Furthermore, the mass transfer area-to-volume ratio is defined by:

$$\frac{A}{V_{0L}} = a_0 \qquad (3\text{-}19)$$

Dividing by V_{Li} and replacing the formula above, one gets

$$\frac{dC_{Li}}{dt} = r_i \frac{m_{cat}}{V_{0L}} - a_0 k_{Li} (c_{Li} - c_{Li}^*) \qquad (3\text{-}20)$$

If the component is non-volatile, the mass transfer coefficient k_{Li} is zero. Moreover, as perfect backmixing of the gas and liquid phases is confirmed in section 6.2 in a tracer experiment, the concentration at the liquid-gas interface c_{Li}^* is calculated by using the Henry's law [14].

For the gas phase mass balance, no reaction is assumed. Therefore, the mass balance of an arbitrary gas-phase component is:

$$N_i A = \dot{n}_{G,out} + \frac{dn_{Gi}}{dt} \qquad (3\text{-}21)$$

3.3.4 Simplified mass balances ($k_{Li} \to \infty$)

As the mass balance for the kinetic modelling requires a simplified equation, simplification was based on the assumption of fast mass transfer and slow reactions, thus reactions in the liquid film can be neglected. As a result, $k_{Li} \to \infty$ and $c_{Li} \to c_{Li}^{*}$. The mathematical simplification follows the treatment of Musakka et al. [14]. The following simplification of mass balance is introduced:

$$\frac{dC_{Gi}}{dt} = \frac{r_i \alpha \frac{m_{cat}}{V_{0L}} - \frac{c_{Gi}\dot{V}_{G,out}(t)}{V_G}}{\frac{\alpha}{K_i} + 1} \qquad (3\text{-}22)$$

where $\alpha = \frac{V_{0L}}{V_G}$, and the relationship between concentrations in gas and liquid phase is described by equilibrium constant K_i. Further information about its calculation is explained in the section 5.1.

As a consequence, the mass balance for gas phase component (CO_2) the equation (3-22) can be verified with a correct reaction mechanism.

For non-volatile components in liquid phase, only the liquid mass balance is applied:

$$\frac{dC_{Li}}{dt} = r_i \frac{m_{cat}}{V_{0L}} \qquad (3\text{-}23)$$

In the developed model, equation (**3-22**) was applied for CO_2 and equation (**3-23**) for other components.

3.4 Kinetic modelling

Kinetic modelling was carried out with the program package MODEST (Model ESTimation), version 6.0. The code is written in standard Fotran 77 [15]. The program was used for parameter estimation. The aim of kinetic modelling was to estimate reaction parameters, such as rate constants and activation energies. In addition, the aim was also to elucidate the hypothetical reaction mechanism, that is presented in the section 6.4.2.

Parameter estimation is a mathematical method that minimizes the difference between model predictions and the experimental results in order to determine the values of unknown parameters. The algorithm uses the least squares estimation, defining an objective function as follows [15]:

$$R^2 = \left(1 - \frac{\left(c_{i,experimental} - c_{i,prdicted}\right)^2}{\left(c_{i,experimental} - \overline{c}_{i,prdicted}\right)^2}\right) * 100 \qquad (3\text{-}24)$$

where, $c_{i,experimental}$ is the experimental concentration value, $c_{i,prdicted}$ is the predicted one and $\overline{c}_{i,prdicted}$ is the average value of all the data points.

An iterative process was applied to determine an optimal value for the parameter to be estimated based on the initial guesses and boundary values provided by the user. This method simultaneously estimates the unknown parameters on two levels: the physical model of the process and the variance model based on the measuring instruments.

The rate constant is described by the Arrhenius law:

$$k = A * e^{\frac{-E_a}{RT}} \qquad (3\text{-}25)$$

To improve statistical analysis equation (**3**-**25**) was rewritten as:

$$k = k_{mean} * e^{\frac{-E_a}{RZ}} \qquad (3\text{-}26)$$

where, $\frac{1}{z} = \frac{1}{T} - \frac{1}{T_{mean}}$ and $k_{mean} = A * e^{\frac{-E_a}{RT_{mean}}}$, being the rate constant at the average temperature T_{mean}.

4 Experimental section

4.1 Experimental set-up description

The reactor operated in two different modes during experiments, a semi-batch mode reactor for the gas phase and a batch mode for the liquid phase. As there are many accessories linked to the reactor, it is important to know how the gas behaves in the system. As a result, the reactor characterization was carried out in the following two ways:

- Volume measurements for the reactor and the condenser
- The tracer experiment

The first part can give a basic idea about the total volume of the reactor and the second one can show the fluid behaviour in the system and the accessible volume occupied by gas phase.

Experiments are carried out under atmospheric pressure. More details are listed in Table 4-1.

Table 4-1 Experiments Conditions and Equipment

	Temperature	Chemicals	Purity	Producer
Volume measurement	24 °C	Deionized water	/	/
Residence time distribution	80 °C (reactor set point)	Deionized water	/	/
		Helium	89%	AGA
		Argon	99.995 %	AGA

4.2 Volume measurement

Since the system has a complex structure (Figure 4-1), it was not possible to obtain an accurate volume of each accessory due to unavailability of reliable data.

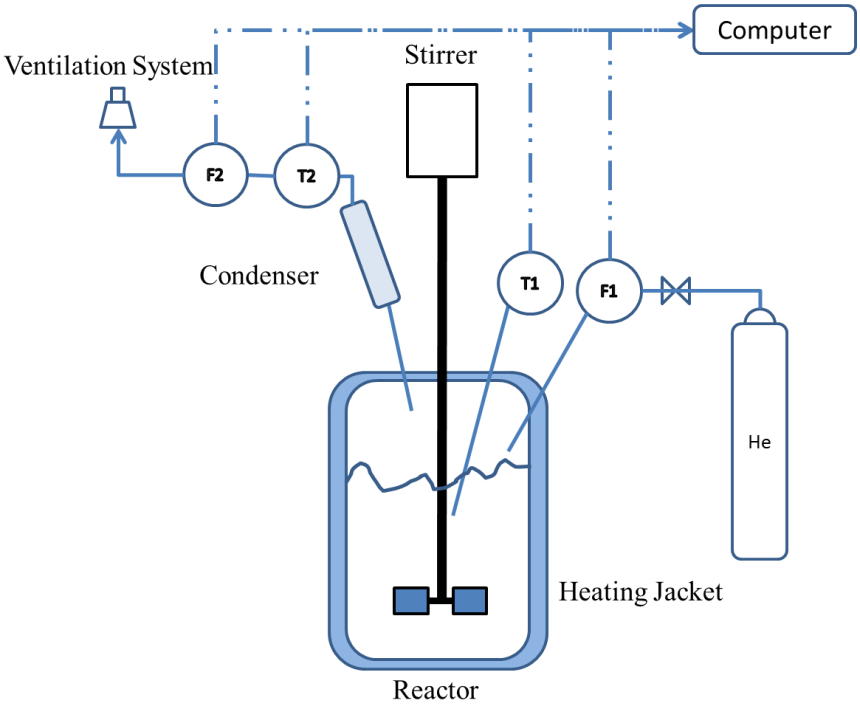

Figure 4-1 System description.

Nevertheless, volumes of the major ones such as the main reactor, condenser and a small connector (see Figure 4-2) can be calculated in the following manner: by filling deionized water in each part of the system and weighing the mass of water to obtain the volume by calculations.

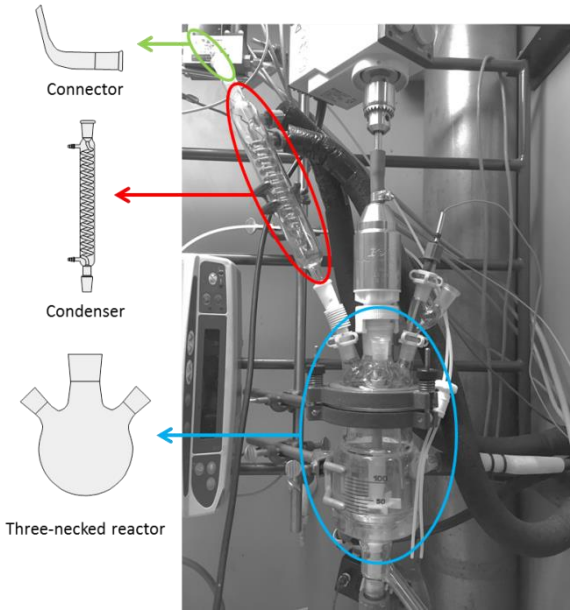

Figure 4-2 System structure and volume measured part.

First, the reactor was washed several times with acetone and deionized water by turning on the stirrer. Then, the reactor is filled with deionized water at room temperature, and then the amount of water was weighted. The total volume is water mass divided by the water density calculated from the literature [16] at room temperature . The water density equation was applied for obtaining a more accurate liquid volume. Density was not considered in modelling of reaction kinetics, because the system is isothermal.

The reactor and the condenser were evaluated in-situ as they were not detachable; the connectors' volume was obtained by taking it out from the system.

4.3 Tracer experiment

Knowing the fluid flow pattern inside the reactor is important for the mass balance, hence a tracer experiment was carried for the gas phase to characterize the gas flow pattern. A pulse tracer experiment was applied in this case. The aim was to determine the residence time distribution and verify the real accessible volume for the gas phase, that is the total volume of the reactor (measured) minus the liquid phase volume (obtained by mass divided by density).

The tracer experiment conditions was selected based on the real experiment conditions, explained in the section 6.4.1.

In this case argon was used as a tracer and helium as a carrier gas. The experiment was performed under the conditions given in Table 4-2:

Table 4-2 Tracer Experiment Conditions

Variable	Location	Values
Temperature [^{o}C]	Gas inlet	24
	Reactor set point	88
	Inside reactor	80
	Condenser	-12
Flowrate [ml/min]	Inlet	15

A system describing the experimental set-up is presented in Figure 4-3.

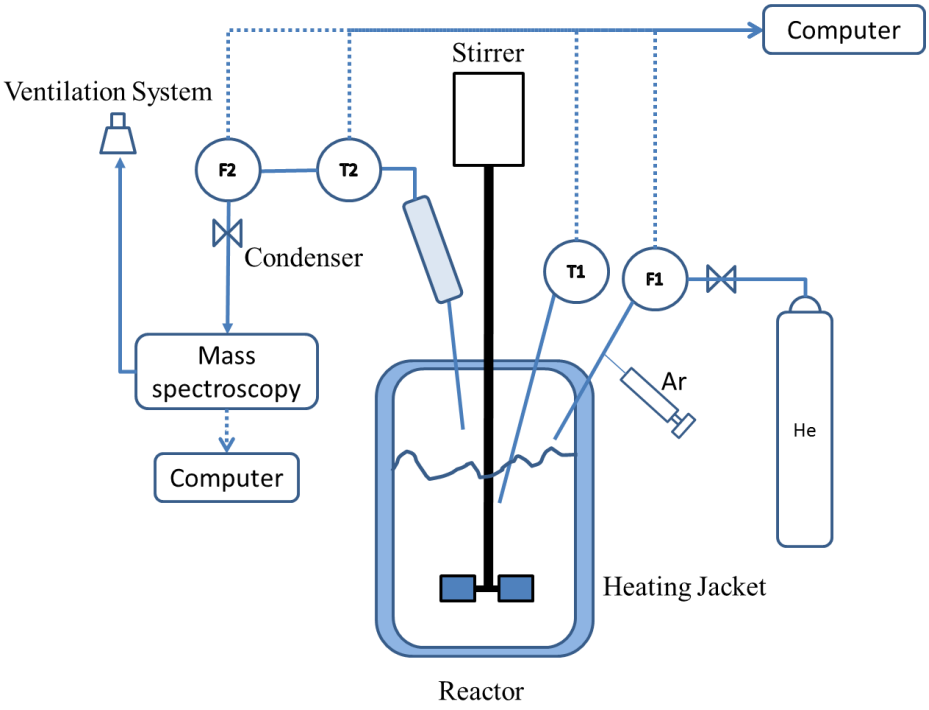

Figure 4-3 Tracer experiment setup.

The reactor was initially rinsed several times with deionized water, thereafter acetone was used for drying.

The reactor was filled with 65 g of deionized water, which it corresponds to the total mass of liquid phase present in catalytic experiments. Afterwards, the reactor was heated to 80 ºC, temperature used in oxidation experiments. The stirrer was turned on and the flow of the carrier gas (helium) commenced. The gas passed through the set-up to be finally analysed by mass spectrometer. Once the system started working, the mass spectrometer was configured to detect possible outlet gases: carbon dioxide, helium, oxygen, nitrogen and hydrogen. Initially, there were atmospheric gases inside of the reactor.

After the helium replaced air and the set, 5 ml of tracer (argon) in a syringe was introduced through the sampling line within a very short time interval setting time t=0. The experiment finished when there was no detected argon at the outlet of the reactor.

5 Calculations and data assessment

5.1 Equilibrium of gas and liquid phases in the system

During the reaction, two main gas components were formed: oxygen and carbon dioxide. Their appearance is related to the rate furfural consumption and other components formation in the system. Therefore, equilibrium of gas and liquid phases of these compounds was studied. However, oxygen was neglected in this case, as its concentration is relatively small compared with carbon dioxide. In addition to this, formation of oxygen is supposed to be linked to decomposition of hydrogen peroxide rather than to other reactions. A detailed study might be needed to confirm this assumption.

Carbon dioxide appeared in larger amounts in comparison to oxygen therefore we have focussed on this reactant, considering:

- The equilibrium constant K_i, which is related to the Henry's law.
- The gas solubility of carbon dioxide in liquid for the verification of the equilibrium constant.

5.1.1 Calculation of the equilibrium constant (K_i)

During the experimental part of this work, which was previously done, two gases were detected in addition to the carrier gas helium: carbon dioxide and oxygen. As mentioned above in comparison with carbon dioxide, the presence of oxygen can be neglected. It is also possible that there were other components present in the gas phase, therefore first boiling points of chemicals appearing in the liquid phase were examined (Table 5-1).

Table 5-1 Boiling Points of Appeared Chemicals in the Liquid Phase

Compound	Boiling point [°C]
2(5)-furanone	86.55 (0.016 atm [17])
Formic acid	100.8 ([18])
Furfural	161.7
Furoic acid	231
Hydrogen peroxide	150.2
Maleic acid	135
Malic acid	225 – 235 ([19])
Malonic acid	140
Succinic acid	235

Formic acid was specially analysed, since its vapour pressure is close to the one for water. Its vapour pressure correlations can be found in hand books [20], revealing that for pure formic acid solution it is higher than for water (compared in Figure 5-1). Nevertheless, the probability of formic acid to escape from the system and get detected in the gas phase is still negligible as the condenser temperature is quite low.

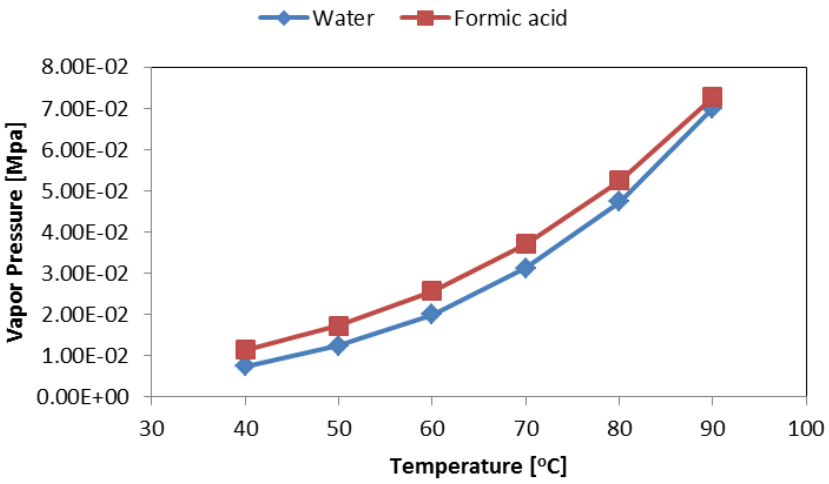

Figure 5-1 Vapour pressure of pure water and formic acid solutions.

There is a possibility that minor amounts of vapours are also present in the gas phase, which is condensed and therefore equilibrium will be attained. To check this hypothesis, a special arrangement for detection is required because the reactor is alredy equiped with too many accessories.

As a result only CO_2 and water were considered. Concentration of carbon dioxide in the liquid phase was calculated theoretically. Using a simple extension of Henry's law [21]:

$$x_{CO_2} H_{21} = y_{CO_2} \hat{\phi}_{CO_2} P_t \qquad (5\text{-}1)$$

where x_{CO_2} is the mole fraction of CO_2 in the liquid, y_{CO_2} is the mole fraction of CO_2 in the vapour, H_{21} is the Henry's constant, $\hat{\phi}_{CO_2}$ is the fugacity coefficient for CO_2 and P_t is the total pressure.

The fugacity coefficient of CO_2 depends on the operating pressure, which at pressures larger than 1 MPa starts to be important. The total pressure here is the atmospheric one, hence the fugacity coefficient can be neglected. The Henry's constant can be calculated by using the following equation [22] :

$$\ln\left(\frac{H_{21}}{MPa}\right) = -6.8346 + \frac{1.2817 * 10^4}{T} - \frac{3.7668 * 10^6}{T^2} + \frac{2.997 * 10^8}{T^3} \qquad (5\text{-}2)$$

The correlation is valid for 273 K < T < 433 K, T is in K.

The Henry's law constant H_{21} can be transformed to K_i by using equations (**3-12**) and (**3-13**). Therefore, K_i is:

$$K_i = \frac{H_{21}}{P_t} \qquad (5\text{-}3)$$

K_i decreases by the temperature increases, since the gas concentration in the liquid phase is lower temperature increase (Figure 5-2).

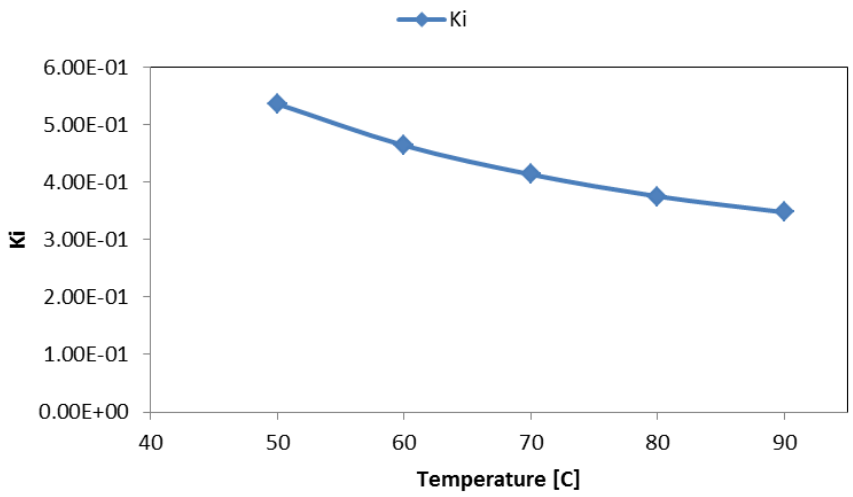

Figure 5-2 Dependence of K_i on temperatures.

5.1.2 Verification of the calculated value of Henry's law constant

Several equations for calculating Henry's law constant were found in the literature survey. However, most of them are really complex like Krichevsky-Kasarnovsky equation [23], and require software packages [24] or further thermodynamic parameters [25]. The equation (5-2 **)** is the most adequate one that can be applied in this case.

Therefore, the verification of the calculated Henry's law constant is based mainly on literature sources. The range of calculated H is around 10^3 MPa increasing with temperature increase. H's values for 0 – 60 °C in atm/mol fraction found in literature [26] are very similar to the calculated ones (Figure 5-3).

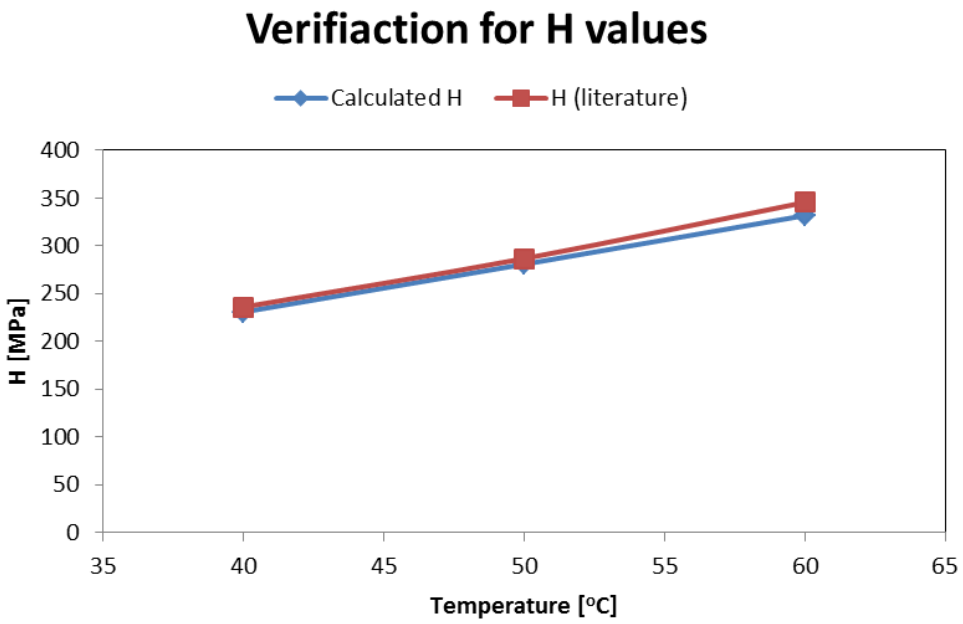

Figure 5-3 Verification for H values.

Solubility of CO_2 in water is also checked. The following equation is applied from 273 K to 353 K [27]:

$$\ln x_g = A + \frac{B}{T} + C \ln\left(\frac{T}{K}\right) + DT \qquad (5\text{-}4)$$

where:

$A = -159.854$

$B = 8742.68\ K$

$C = 21.6694$

$\mathrm{D} = -1.10261 * 10^3\ K^{-1}$

Since the mole fraction in the liquid phase of the system calculated by the Henry's law is much lower than the one calculated with the above correlation.

5.2 Data assessment (change of units)

The primary data for the gas phase was in volume percentage (V%) and the liquid phase with unit in weight percentages. Unit changing was required so that can be able to apply rate equations and the mass balances (section 3.3), which are based on concentrations. According to the definition of the concentration:

$$c_i = \frac{n_i}{V_t} \qquad (5\text{-}5)$$

For the liquid phase, V_t is the total volume of the solution. In a major part of experiments, the water has a weight percentage more than 90%, so others compounds' concentration have relatively small contribution to density in comparison to it. Therefore, only water's volume is considered:

$$V_{t,L} = m_w \rho_w \qquad (5\text{-}6)$$

And the molar number of each species can be obtained by the next equation:

$$n_i = \frac{wt\%_i * m_{total}}{100 * M_i} \qquad (5\text{-}7)$$

where, M_i is the molecular mass of each component (see in the Appendix II).

In the gas phase, V_t is the total volume of gas phase that means:

$$V_{t,g} = \frac{n_t * R * T}{P_t} \qquad (5\text{-}8)$$

As in gas phase, the molar fraction is equal to the volume fraction, and the molar percentage in a gas system is equal to the volume percentage, so the following expression of c_i is obtained:

$$c_i = \frac{n_i}{V_{t,g}} = \frac{vol\%}{100} * \frac{P_t}{R * T} \qquad (5\text{-}9)$$

The above formula was used for the unit change for the Modest data sets and it was only applied for carbon dioxide, since it was present in the liquid and gas phase.

6 Results and discussion

6.1 Volume measurement

Dividing deionized water mass by density, the volume can be calculated:

$$V_w = \frac{m_w}{\rho_w} \qquad (6\text{-}1)$$

where, V_w is water volume, m_w the weighted mass and ρ_w is water density at room temperature being 0.962 g/ml, calculated from the correlation given by McCutheon et al.[16].

The obtained volumes are shown in the Table 6-1:

Table 6-1 Measured Volumes

	Deionized water mass [g]	Volume [ml]
Connector	5.66	5.66
Condenser	89.98	90.02
Reactor	403.08	403.25

6.3 Residence time distribution

The response from the mass spectrometry in Amperes was normalized in a way that the maximum was equals to unity, by applying the following equation:

$$I_{normalized} = \frac{I(t)}{I_{initial}} + 1 \qquad (6\text{-}2)$$

Therefore, the Figure 6-1 was obtained.

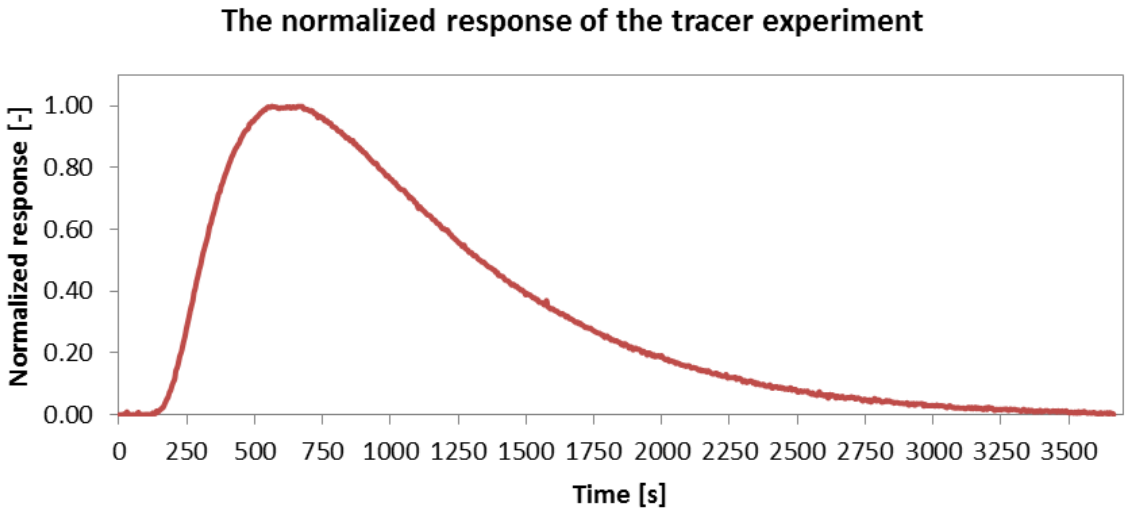

Figure 6-1 The normalized response of the pulse tracer experiment.

From Figure 6-1, the average residence time ($\bar{t}$) can be determined as time when the response reaches the maximum value. The objective is to compare the observed value with the expected value of the holding residence time. The analysis of the tracer experiment response is presented in Figure 6-2.

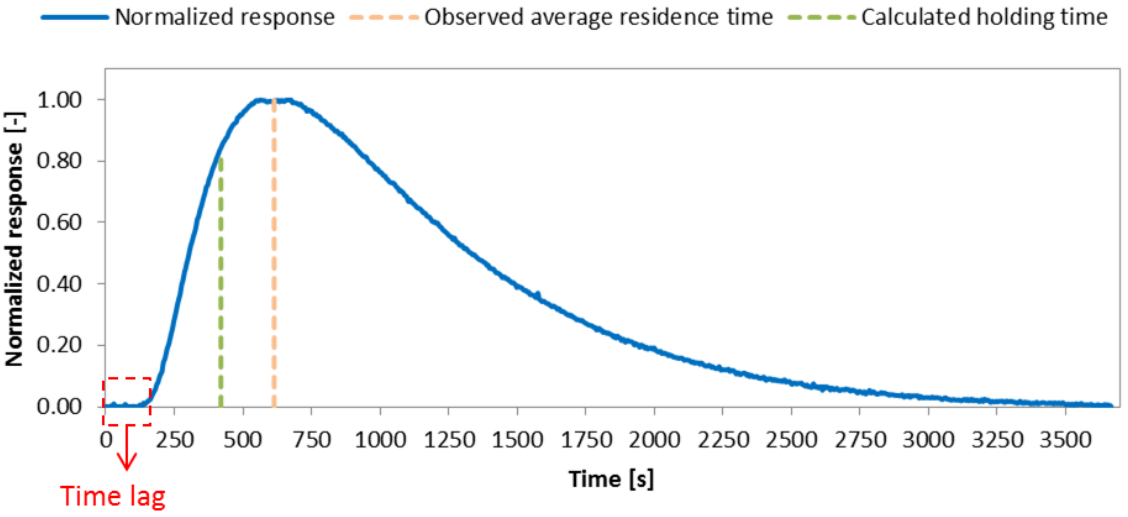

Figure 6-2 Tracer experiment response analysis.

In Figure 6-2, time lag of circa 120 seconds was observed. This implies plug flow in series with a mixed flow to the condenser and the connector [9].

If the accessible volume of the gas phase is assumed equal to the total one, the holding time (**3**-**3**),can be calculated according to equation (**3**-**5**), thus the total accessible volume is:

$$V_G = V_R - V_L \qquad (6\text{-}3)$$

where, V_G is the reactor volume for the gas, V_R the reactor volume and V_L the liquid phase volume.

For the inlet gas flowrate being 15 ml/min at 24 °C, the temperature influence for the gas phase should be considered:

$$\frac{V_1}{T_1} = \frac{V_2}{T_2} \qquad (6\text{-}4)$$

Giving the gas flowrate of 50 ml/min at 80 °C.

Furthermore, the time delay can be assumed as a combined effect of the connector and the condenser and using equation (**3**-**3**) resulting in:

$$t_{delay} = \frac{V_{condenser+connector}}{\nu} \qquad (6\text{-}5)$$

By changing the gas volume flowrate in seconds, the values were obtained, as presented in Table 6-2 and Table 6-3.

Table 6-2 Calculated Time Delay caused by Condenser and Connector

	Volume [ml]	$t_{delay}\ [s]$
Connector	5.66	6.79
Condenser	90.02	107.97
	Sum	114.76

Table 6-3 Comparison of Calculated and Observed Residence Time

	$t_{delay}\ [s]$	$\bar{t}_R [s]$
Observed value	123.73	490.20
Calculated value	114.76	402.82

$\bar{t}_R$ is the average residence time for the reactor, which does not include the delay time in the system. Since there is no adsorption phenomena in gas phase, the average residence time is equal to the holding time (see section 3.1.1) [7].

Observed values are obtained from the response of the system and calculated values came from the equation (**3**-**3**) in the approximation that the reactor is a perfectly back-mixed one.

In both cases, the observed value is larger than the calculated. One of the possible reasons is that there may be a time delay due to the mass spectrometer measurements: which needs time to analyse the gas flux and also it requires time to transport the gas.

Nevertheless, the gas pipe volume (Figure 6-3, red lines) was not measured due to the small diameter is really small, thus the pipe volume was neglected.

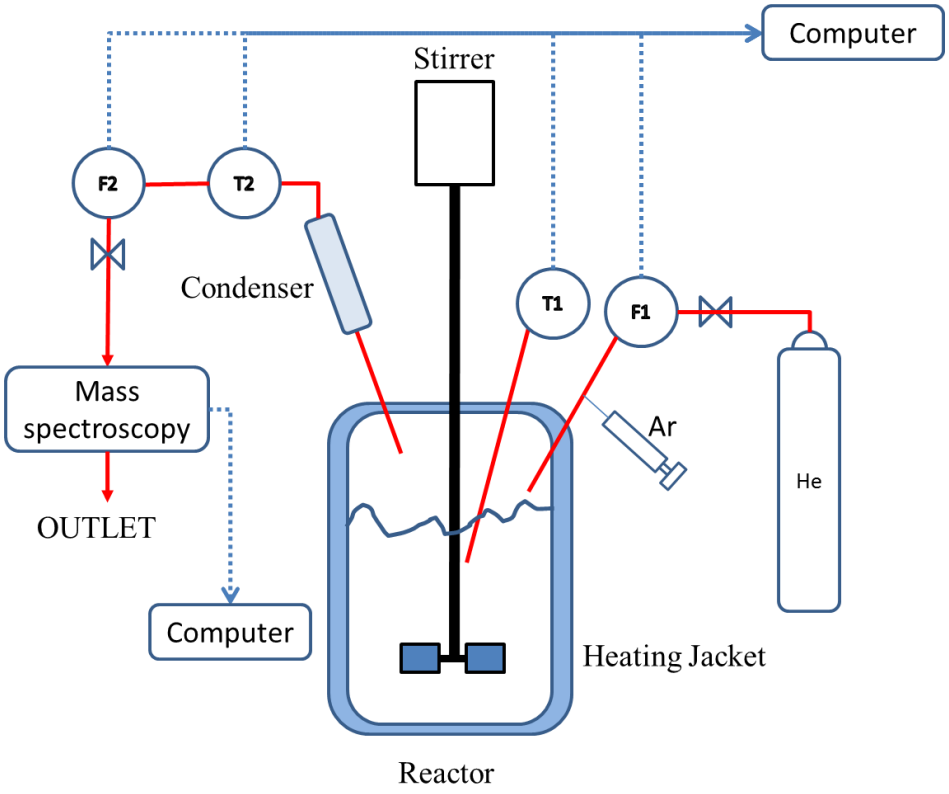

Figure 6-3 Red lines are neglected parts in the volume measurement.

6.4 Kinetic modelling and data assessment

6.4.1 Experiment data sets description

19 experiments were carried out previously a Laboratory of Industrial Chemistry, varying the following parameters were varied:

- Temperature (from 40 – 90 ^{o}C).
- Molar ratio of hydrogen peroxide to furfural (2-8).
- Weight percentage of catalyst to furfural (10%, 25% and 50%).
- Weight percentage of the initial concentration of furfural (2.6%, 4.5%, 6.7%).

All the reactions were conducted under atmospheric pressure. An overview of each reaction conditions is given in Table 6-4:

Table 6-4 Summary of Reaction Conditions

Temperature [^{o}C]	Molar ratio (HP/F)	Weight %* (Cat/F)	Initial concentration of F (wt %)
40, 50, 60, 70, 90	3	50	4.5
80	4	50	2.6, 4.5, 6.7
	4	10, 25	4.5
	2, 2.5, 3, 4, 5, 6, 7, 8	50	4.5

*: 1.5 g of catalyst for 50%, 0.75 g for 25% and 0.3 g for 10%

Although there were 19 experiments, only a part of them was analysed with software Modest. Namely 14 sets were analysed, in some data sets there were non-measured variables (e.g. gas concentrations at 40 ^{o}C). Analyzed experimental data conditions are given in Table 6-5.

Table 6-5 Reaction Conditions for Analyzed Experimental Data

Temperature [^{o}C]	Molar ratio (HP/F)	Weight %* (Cat/F)	Initial concentration of F (wt %)
60, 70	3	50	4.5
80	4	50	2.6, 4.5, 6.7
	4	10, 25	4.5
	2, 2.5, 3, 4, 5, 6, 7, 8	50	4.5

6.4.2 Reaction mechanism hypothesis and rate expressions

Oxidation of furfural generates a range of products, by-products and intermediates during the reaction making it difficult to estimate with statistical significance all the kinetic parameters. Therefore, before estimation of kinetic parameters different assumptions were made to check which hypothesis can explain better the experimental data. After an initial literature search, none of the reaction mechanisms described in the literature matched the experimental observations. Therefore, a hypothesis of the reaction steps was made giving a very simplified version (Figure 6-4). It should be emphasized that there are many other reactions also taking place which are not mentioned here.

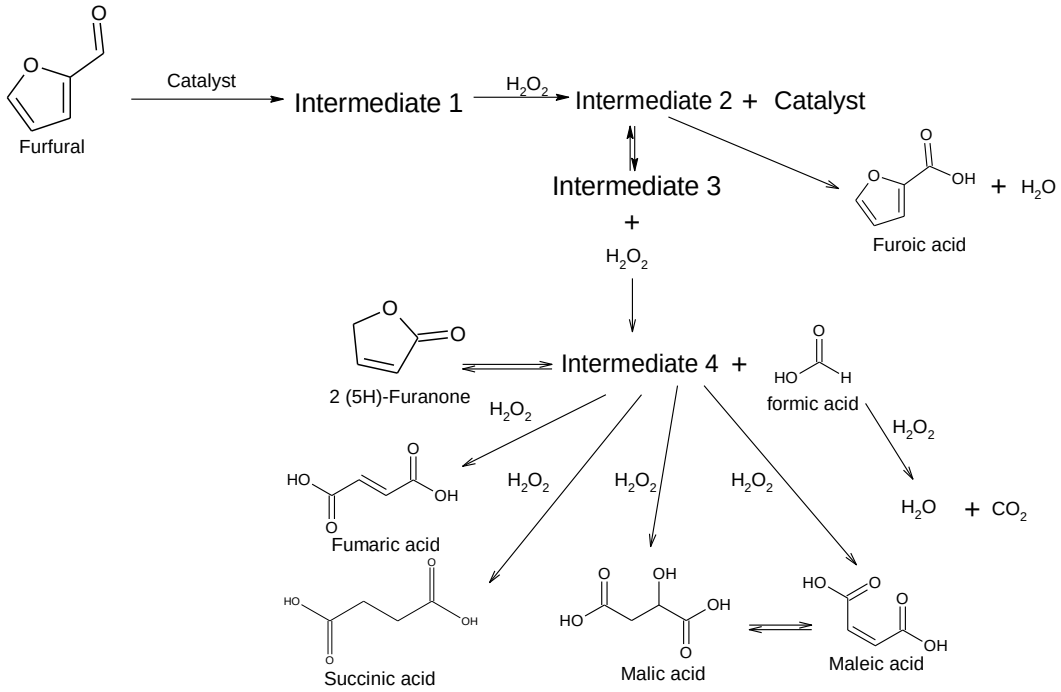

Figure 6-4 Simplified version of reaction mechanism hypothesis.

Reaction steps are listed in Table 6-6:

Table 6-6 Hypothetical Reaction Mechanism

Reaction steps	Step number
$F + cat = I_1$	(1)
$I_1 + HP = I_2 + cat$	(2)
$I_2 = I_3 + w$	(3)
$I_2 \rightarrow FurA + w$	(4)
$I_3 + w = I_4 + FoA$	(5)
$I_4 = Hf$	(6)
$FoA + HP \rightarrow CO_2 + w$	(7)
$I_4 + HP \rightarrow Mi$	(8)
$I_4 + HP \rightarrow SA$	(9)
$I_4 + HP \rightarrow FumA$	(10)
$I_4 + HP \rightarrow Me$	(11)
$FumA = Me$	(12)

Chemical abbreviations in Table 6-6 are explained in Nomenclature, I_i represents unknown intermediate species. Final products are: furoic acid (FurA), formic acid (FoA), carbon dioxide (CO_2), 2-(5H) furanone (Hf), malic acid (Mi), succinic acid (SA), fumaric acid (FumA) and maleic acid (Me).

In step (1) furfural carbonyl carbon is protonated by the acidic catalyst and the intermediate I_1 is formed. Then the intermediate reacts with hydrogen peroxide in the rate determining step forming I_2. I_2 forms at the same time water, furoic acid and a new intermediate specie: I_3. After the reaction between water and I_3, formic acid and I_4 are generated. Step (6) is isomerization to 2(5H)-furanone. Finally formic acid and I_4 are oxidized to other lower carbon number components. Step (12) is isomerization of fumaric acid to maleic acid.

As a primary approximation, intermediates were considered to be consumed immediately after their generation, meaning:

$$\frac{dI_i}{dt} = rate\ of\ generation - rate\ of\ consumption = 0 \qquad (6\text{-}6)$$

For $= 1,2,3,4$.

By applying equation (**6**-**6**) for every intermediate:

$$\frac{dI_1}{dt} = r_{+1} - r_{-1} - r_{+2} + r_{-2} = 0 \qquad (6\text{-}7)$$

$$\frac{dI_2}{dt} = r_{+2} - r_{-2} - r_{+3} + r_{-3} - r_4 = 0 \qquad (6\text{-}8)$$

$$\frac{dI_3}{dt} = r_{+3} - r_{-3} - r_{+5} + r_{-5} = 0 \qquad (6\text{-}9)$$

$$\frac{dI_4}{dt} = r_{+5} - r_{-5} + r_{-6} - r_{+6} - r_8 - r_9 - r_{10} - r_{11} = 0 \qquad (6\text{-}10)$$

By writing the expression of each rate, with k_{i+} being the forward and k_{i-} the reverse rate constant for the formation of reactant (from right to left), rate expressions are listed in Table 6-7:

Table 6-7 Rate Expression in each Reaction

r_i	Expression	r_i	Expression
r_{+1}	$k_{+1}c_F c_{cat}$	r_{+6}	$k_{+6}I_4$
r_{-1}	$k_{-1}I_1$	r_{-6}	$k_{-6}c_{Hf}$
r_{+2}	$k_{+2}I_1 c_{HP}$	r_7	$k_7 c_{FoA} c_{HP}$
r_{-2}	$k_{-2}I_2 c_{cat}$	r_8	$k_8 I_4$
r_{+3}	$k_{+3}I_2$	r_9	$k_9 I_4$
r_{-3}	$k_{-3}I_3 c_w$	r_{10}	$k_{10}I_4$
r_4	$k_4 I_2$	r_{11}	$k_{11}I_4$
r_{+5}	$k_{+5}I_3 c_w$	r_{+12}	$k_{+12}c_{FumA}$
r_{-5}	$k_{-5}I_4 c_{FoA}$	r_{-12}	$k_{-12}c_{Me}$

To obtain the concentrations of intermediates expressions in equations (**6**-**7**) - (**6**-**10**), are rearranged:

$$I_2 = \frac{I_1(k_{-1} + k_{+2}c_{HP}) - k_{+1}c_F c_{cat}}{k_{-2}c_{cat}} \quad (6\text{-}11)$$

$$I_3 = I_1\frac{A}{c_w} - \frac{k_{+1}c_F(c_{cat}k_{-2} + k_4)}{c_w k_{-2}k_{-3}} \quad (6\text{-}12)$$

$$I_4 = \frac{I_2 k_{+3} + I_3 c_w(k_{-3} - k_{+5})}{c_{FoA}k_{-5}} \quad (6\text{-}13)$$

The following step is to incorporate equations (**6**-**11**) and (**6**-**12**) into (**6**-**13**), giving:

$$I_1 = \frac{c_{Hf}k_{-2}k_{-3}k_{-6} - k_{-3}k_{+1}\gamma - k_{+1}k_{+5}c_F(1-\gamma)(k_4 + k_{-2}c_{cat})}{k_{-3}\left(\beta k_{-2}c_{cat}(k_{-3} - 2k_{+5}) + k_{+3}(k_{-1} + c_{HP}k_{-2})\right)} \quad (6\text{-}14)$$

In the equation (**6**-**14**), β and γ are abbreviations for:

$$\beta = \frac{k_{-1}k_{-2}c_{cat} + k_{-1}k_{+3} + k_{+3}k_{+2}c_{HP}}{c_{cat}k_{-2}k_{-3}}$$

$$\gamma = \frac{k_{6+} - k_{-5}c_{FoA} - c_{HP}\left(\sum_{i=8}^{i=11} k_i\right)}{c_{FoA}k_{-5}}$$

Finally, the generation equation for each compound can be written:

$$\frac{dc_F}{dt} = r_{+1} - r_{-1} \quad (6\text{-}15)$$

$$\frac{dc_{HP}}{dt} = r_{-2} - r_{+2} - (r_7 + r_8 + r_9 + r_{10} + r_{11}) \quad (6\text{-}16)$$

$$\frac{dc_{FurA}}{dt} = r_4 \quad (6\text{-}17)$$

$$\frac{dc_{FoA}}{dt} = r_{+5} - r_{-5} - r_7 \quad (6\text{-}18)$$

$$\frac{dc_{Hf}}{dt} = r_{+6} - r_{-6} \quad (6\text{-}19)$$

$$\frac{dc_{Mi}}{dt} = r_8 \quad (6\text{-}20)$$

$$\frac{dc_{SA}}{dt} = r_9 \quad (6\text{-}21)$$

$$\frac{dc_{FumA}}{dt} = r_{10} - r_{12+} + r_{-12} \qquad (6\text{-}22)$$

$$\frac{dc_{Me}}{dt} = r_{11} \qquad (6\text{-}23)$$

$$\frac{dc_{w}}{dt} = r_{+3} - r_{-3} + r_{4} + r_{7} \qquad (6\text{-}24)$$

$$\frac{dc_{CO2}}{dt} = r_{7} \qquad (6\text{-}25)$$

6.4.3 Kinetic modelling

In section 6.4.1, a possible reaction mechanism is discussed, which still needs an improvement. As already discussed, there are many steps and hence a simpler reaction mechanism was applied for modelling using the optimization software Modest. The Model structure of variables is shown in Table 6-8.

Table 6-8 Used Variables in Modest

Modest variables types	Variables
Observed variables	Concentrations $c_i(t)$
Local variables	Intial liquid volume (V_L) Temperature (T) Catalyst mass (m_{cat}) Equilibrium constant (K_i)
Control variables	Outlet gas flowrate ($\dot{V}_{G,out}(t)$)
Estimated variables	Average rate constant ($\bar{k}_i$) Activation energies (E_{ai})

A simplified scheme of the workflow of it is presented in Figure 6-5.

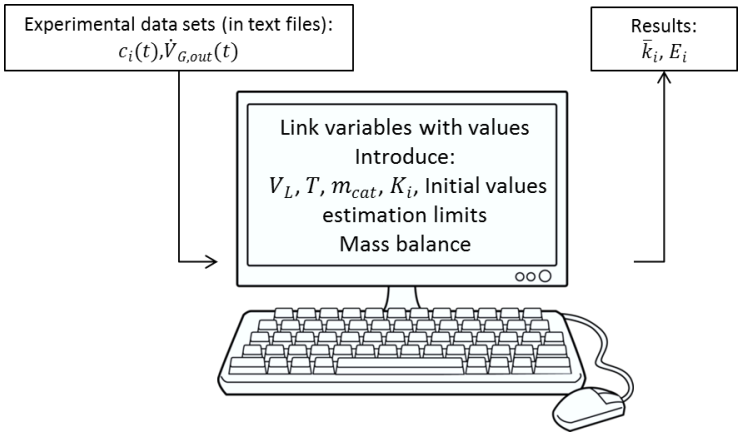

Figure 6-5 Workflow procedure with software Modest.

It is clear that it could be difficult to precisely account for all data sets in kinetic modelling if the reaction mechanism is not well understood. However, it is always possible to analyze the tendens in formation and consumption of.

For example, from the trend of formic acid concentration, it is clear that there are consecutive reactions with formation and subsquent dissapearence of this acid (Figure 6-6). A possible product of formic acid reaction with hydrogen peroxide should be CO_2.

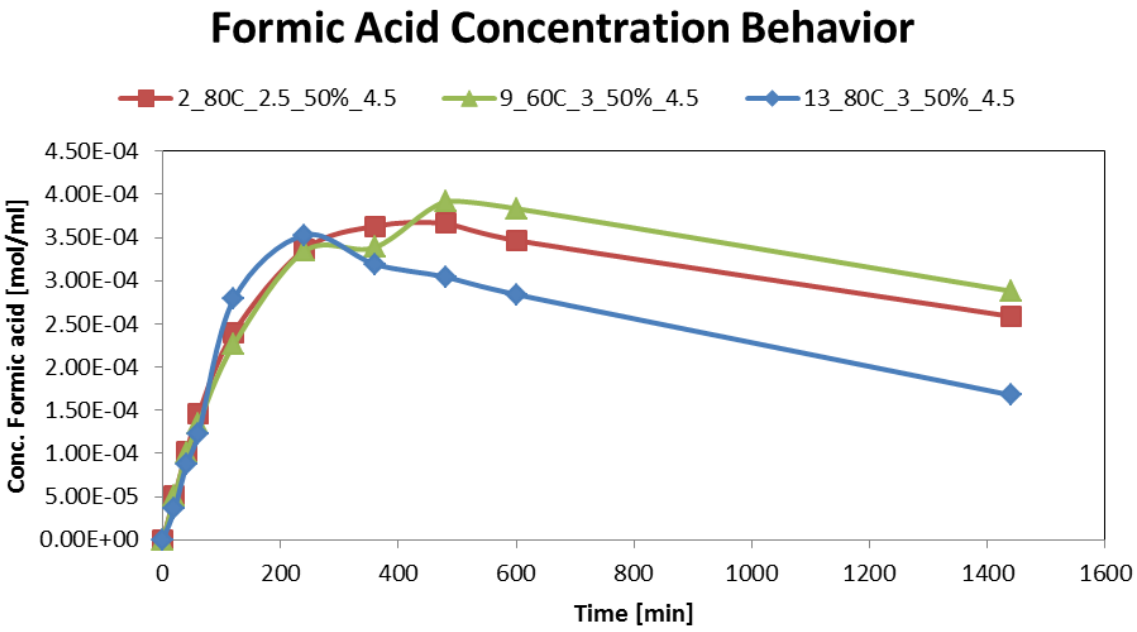

Figure 6-6 Formic acid concentration profile.

The aim of kinetic modelling in this thesis was to describe mainly furfural and formic acid concentration profiles, there are many uncertainties in the reaction network, making it quite challenging to model concentration dependences of various intermediates. To this end, two alternative assumptions were considered.

Assumption 1

In this case, formation of I_4 and formic acid occurred at the same time giving I_4 in equimolar amounts with formic acid. Therefore the measured concentration of formic acid is approximatly the same as the concentration of the intermediate:

$$c_{FoA} \cong c_{I_4} = c_{Mi} + c_{Me} + c_{SA} + c_{Hf} + c_{FumA} \qquad (6\text{-}26)$$

Moreover, formic acid is also formed from other reactions in addition to simultaneous reaction with I_4. The concentration variations for formic acid can be oberved in Figure 6-7. The concentration of formic acid reached maximum, then it decreased and gets close to zero. The formic acid concentrations formed from other reactions ($c_{FoA'}$) were calculated by the expression (**6-27**).

$$c_{FoA'} = c_{FoA,measured} - (c_{Mi} + c_{Me} + c_{SA} + c_{Hf} + c_{FumA}) \qquad (6\text{-}27)$$

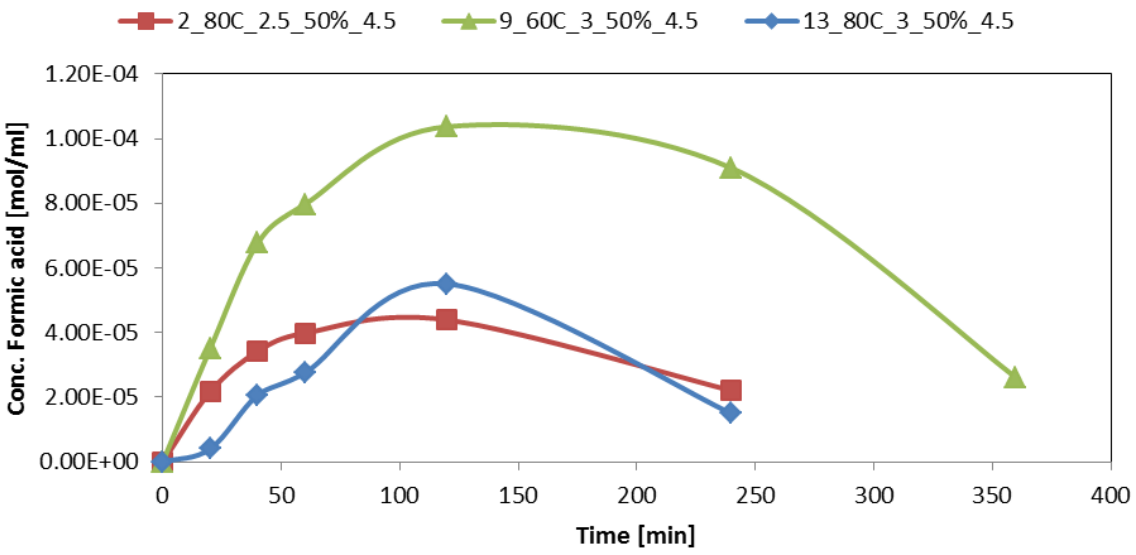

Figure 6-7 Formic acid formation (not simultaneous as I_4) concentration behaviour.

Thus, the reaction mechanism applied for kinetic modelling is the one given in Table 6-9:

Table 6-9 Reaction Mechanism Applied for Kinetic Modelling (Assumption 1)

Reaction steps	Step number
F + HP + cat = FurA	(1)
F → FoA	(2)
F + HP + cat → Hf	(3)
FoA + HP → CO_2	(4)
I_4 + HP → Mi	(5)
I_4 + HP → SA	(6)
I_4 + HP →FumA	(7)
I_4 + HP →Me	(8)
FumA = Me	(9)

This mechanism is simpler in comparison to Table 6-6. Here the concentration of water is not explicitly used because of the following reason: the water participates in elementary reaction steps being in large excess. In addition, several quasi-equilibria in the previous hypothesis were ignored.

Nevertheless, this assumption is based on the previous one: protonation of furfural and the reaction with protonated hydrogen peroxide occur in the same step. As it was assumed previously in (**6**-**26**), the amount of this intermediate is similar to formic acid concentration, therefore in the model, formic acid concentration was used instead of it. According to the reaction steps in Table 6-9, the rate expressions for each compound should be:

$$r_{FurA} = k_1 c_F c_{HP} c_{cat} \qquad (6\text{-}28)$$

$$r_{Hf} = k_3 c_F c_{HP} c_{cat} \qquad (6\text{-}29)$$

$$r_{CO2} = k_4 c_{FoA} c_{HP} \qquad (6\text{-}30)$$

$$r_{Mi} = k_5 c_{I_4} c_{HP} = k_5 c_{FoA} c_{HP} \qquad (6\text{-}31)$$

$$r_{SA} = k_6 c_{I_4} c_{HP} = k_6 c_{FoA} c_{HP} \qquad (6\text{-}32)$$

$$r_{FumA} = k_7 c_{I_4} c_{HP} - k_{+9} c_{FumA} + k_{-9} c_{Me} = k_7 c_{FoA} c_{HP} - k_{+9} c_{FumA} + k_{-9} c_{Me} \qquad (6\text{-}33)$$

$$r_{Me} = k_8 c_{I_4} c_{HP} + k_{9+} c_{FumA} - k_{9-} c_{Me} = k_8 c_{FoA} c_{HP} + k_{9+} c_{FumA} - k_{9-} c_{Me} \qquad (6\text{-}34)$$

$$r_{ForA} = k_2 c_F - r_{CO2} - r_{Mi} - r_{SA} - c_{FoA}(k_7 + k_8) \qquad (6\text{-}35)$$

$$r_F = -r_{Hf} - r_{FurA} - k_2 c_F \qquad (6\text{-}36)$$

$$r_{HP} = -r_{Hf} - r_{FurA} - r_{CO2} - r_{SA} - r_{Mi} - (k_7 + k_8) c_{FoA} c_{HP} \qquad (6\text{-}37)$$

Assumption 2:

In this assumption intermediate I_4 is not formed, and furfural reacts directly to malic, maleic, succinic, fumaric acids and 2(5H) furanone, furthermore formic acid forms in the same amount as these components. This hypothesis is based on the fact that products have one less carbon than the reactants. Then, the amount of formic acid formed from other reactions follow equation (**6-27**). The reaction mechanism applied for kinetic modelling is the correspond to the one presented in Table 6-10:

Table 6-10 Reaction Mechanism Applied for Kinetic Modelling (Assumption 2)

Reaction steps	Step number
F + HP + cat = FurA	(1)
F → FoA	(2)
F + HP → Hf	(3)
FoA + HP → CO_2	(4)
F + HP → Mi + FoA	(5)
F + HP → SA + FoA	(6)
F + HP →FumA + FoA	(7)
F + HP →Me + FoA	(8)
FumA = Me	(9)

According to the reaction steps in Table 6-10, the rate expressions of each compound should be:

$$r_{FurA} = k_1 c_F c_{HP} c_{cat} \quad (6\text{-}38)$$

$$r_{Hf} = k_3 c_F c_{HP} \quad (6\text{-}39)$$

$$r_{CO2} = k_4 c_F c_{HP} \quad (6\text{-}40)$$

$$r_{Mi} = k_5 c_F c_{HP} \quad (6\text{-}41)$$

$$r_{SA} = k_6 c_F c_{HP} \quad (6\text{-}42)$$

$$r_{FumA} = k_7 c_F c_{HP} - k_{9+} c_{FumA} + k_{9-} c_{Me} \quad (6\text{-}43)$$

$$r_{Me} = k_8 c_F c_{HP} + k_{9+} c_{FumA} - k_{9-} c_{Me} \quad (6\text{-}44)$$

$$r_{ForA} = k_2 c_F - r_{CO2} + r_{Mi} + r_{SA} + c_F(k_7 + k_8) \quad (6\text{-}45)$$

$$r_F = -k_2 c_F - r_{Mi} - r_{SA} - r_{Hf} - c_F(k_7 + k_8) \quad (6\text{-}46)$$

$$r_{HP} = -r_{Hf} - r_{FurA} - r_{CO2} - r_{SA} - r_{Mi} - (k_7 + k_8) c_{FoA} c_{HP} \quad (6\text{-}47)$$

Detailed model codes in Modest can be found in Appendix I.

By running both models the following results were obtained. First, in both cases the concentration of furfural is well-described for temperature range 60 – 80 °C with better results achieved at lower temperature (Figure 6-8).

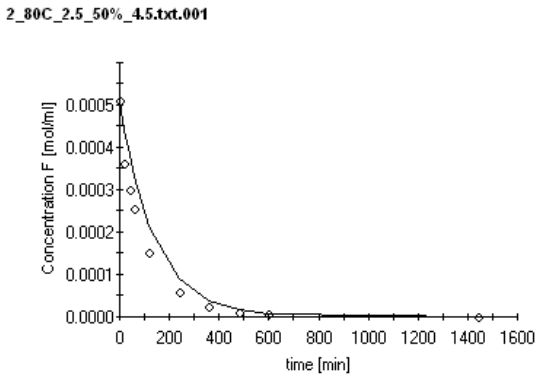

a. T=80 °C, HP/F = 2.5, cat/F=50%

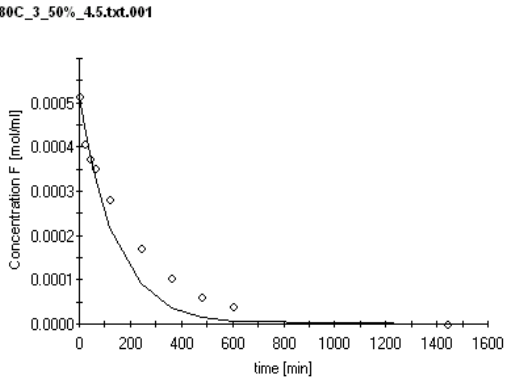

b. T=80 °C, HP/F = 3, cat/F=50%

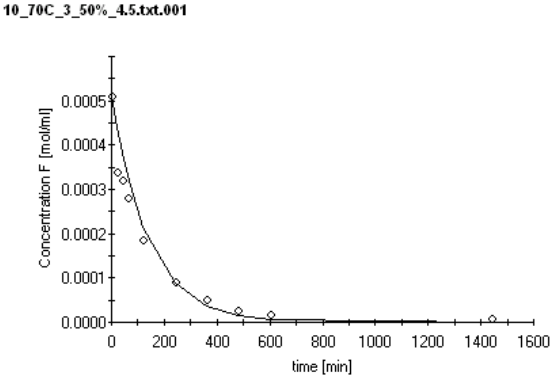

c. T=70 °C, HP/F = 3, cat/F=50%

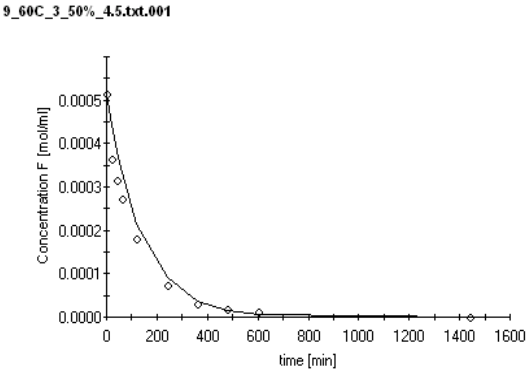

d. T=60 °C, HP/F = 3, cat/F=50%

Figure 6-8 Modelling results of furfural consumption.

However, when the molar ratio HP/F is more than 3, calculated values are far away from the experimental results (Figure 6-9):

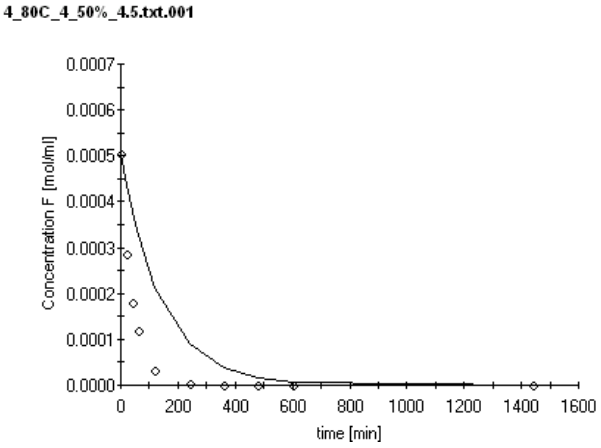

a. T=80 °C, HP/F = 4, cat/F=50%

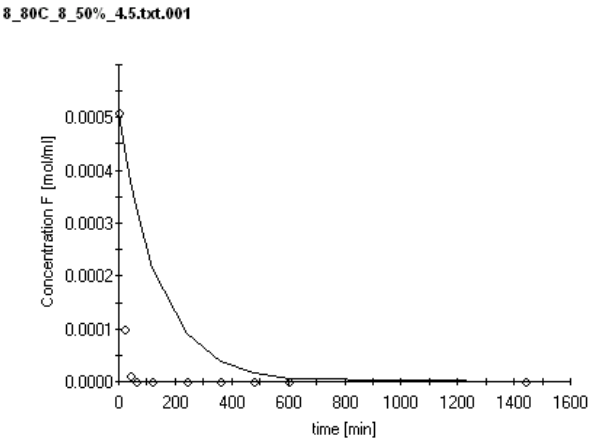

b. T=80 °C, HP/F = 8, cat/F=50%

Figure 6-9 Modelling results of furfural consumption for molar ratio HP/F is higher than 3.

Those results show that higher is the molar ratio, larger is the estimation error. A possible reason of this error is that the reaction order in hydrogen peroxide is above unity, which is not considered in the simplified mechanism. Therefore, a more detailed study is needed to improve the model.

On the other hand, the existence of the intermediate species for the assumption 1. The comparison is presented in Figure 6-10, where only formic acid and furfural experimental and estimated concentrations are plotted.

Assumption 1	Assumption 2
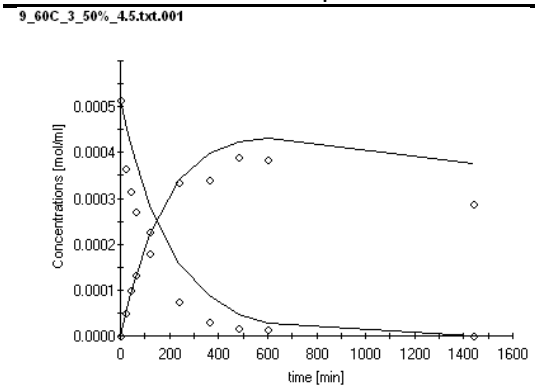	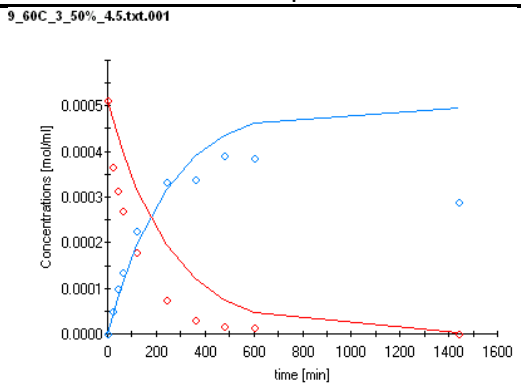
a. T=60 °C, HP/F = 3, cat/F=50%	
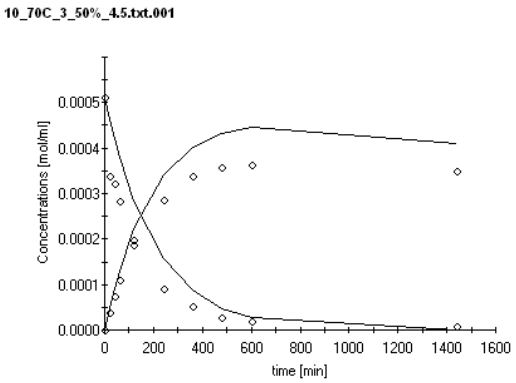	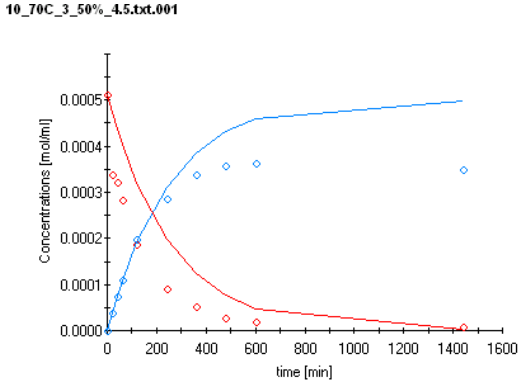
b. *T=70 °C, HP/F = 3, cat/F=50%*	
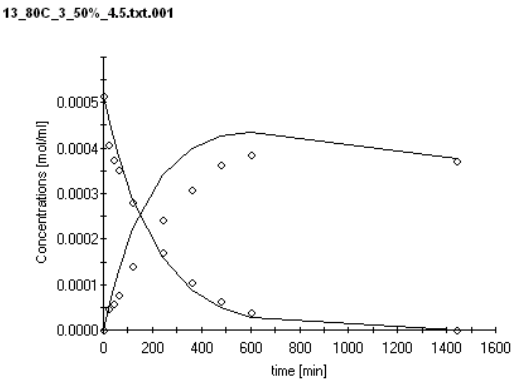	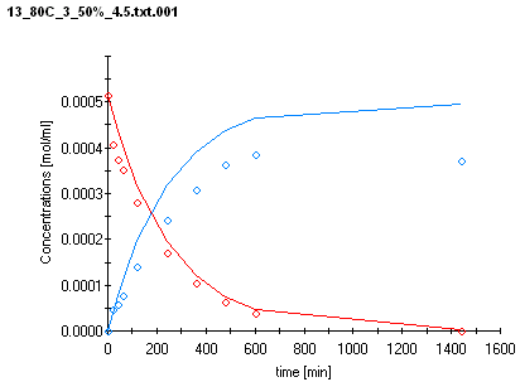
c. T=80 °C, HP/F = 3, cat/F=50%	

Figure 6-10 Result Comparison between Assumption 1 and 2

According to Figure 6-10, it is obvious that assumption 1 corresponds better to experimental data than assumption 2. In particular, the concentration of formic acid in assumption 2 is much higher than experimental data recorded. For the assumption 1 the concentration of formic acid decreases, following the trend of experimental concentrations.

As a conclusion, it can be stated that there is an intermediate involved in the formation of formic acid from other routes.

6.5 Conclusions and outlook

Behaviour of the reactor was verified by RTD experiments confirming that the reactor can be treated as a completely back-mixed one.

The gas-liquid equilibrium of CO_2 was studied and verified. More accurate equations can be used for describing this equilibrium that the ones used in the current thesis.

By kinetic modelling the existence of a key intermediate species was confirmed. It is an intermediate that has concentration close to concentration of formic acid. Thus, those compounds are generated also in a same reaction simultaneously. Formic acid is generated from other reactions. At the same time, the intermediate can react with hydrogen peroxide to produce CO_2. Kinetic modelling showed very good correspondence with experimental data for furfural consumption, however, poor description of data at high hydrogen peroxide concentration calls for a further improvement of the reaction mechanism.

Appendix I

Modest model code for the simplified reaction mechanism:

Assumption 1

```
cMe=s(1) !Maleic acid

cMi=s(2) !Malic acid

cMo=s(3) !Malonic acid

cSA=s(4) !Succinic acid

cHP=s(5)!H2O2

cFoA=s(6) !Formic acid

cFumA=s(7) !Fumaric acid

cHf=s(8) !2(5)H furanone

cFurA=s(9) !Furoic acid

cF=s(10) !Furfural

cCO2=s(11) ! CO2 in gas phase


Temp=Tempc+273.15d0

Tmean=Tmeanc+273.15d0


z=1.0d0/Temp-1.0d0/Tmean

k1=km1*exp(-E1/8.3143d0*z)

k2=km2*exp(-E2/8.3143d0*z)

k3=km3*exp(-E3/8.3143d0*z)

k4=km4*exp(-E4/8.3143d0*z)

k5=km5*exp(-E5/8.3143d0*z)

k6=km6*exp(-E6/8.3143d0*z)

k7=km7*exp(-E7/8.3143d0*z)
```

```
k8=km8*exp(-E8/8.3143d0*z)

k9=km9*exp(-E9/8.3143d0*z)

k9r=km9r*exp(-E9r/8.3143d0*z)


vr=403.245d0

vg=vr-vl

rhoc=mcat/vl

alpha=vl/vg


rFurA=k1*cF*cHP*rhoc

rSA=k6*cFoA*cHP

rHf=k3*cF*cHP

rMe=k8*cFoA*cHP+k9*cFumA-k9r*cMe

rFumA=cFoA*cHP*k7+k9r*cMe-k9*cFumA

rMi=cFoA*cHP*k5

rCO2=k4*cFoA*cHP

rFoA=k2*cF-rCO2-rMi-rSA-cFoA*cHP*(k7+k8)

rF=-rFurA-rHf-k2*cF

rHP=-rco2-rFurA-rSA-rMi-(k8+k7)*cFoA*cHP-rHf


ds(1)=rMe

ds(2)=rMi

ds(3)=0.0d0

ds(4)=rSA

ds(5)=rHP

ds(6)=rFoA
```

```
ds(7)=rFumA

ds(8)=rHf

ds(9)=rFurA

ds(10)=rF

ds(11)=(rCO2*alpha-cCO2*vout/vg)/((alpha/ki)+1)
```

Assumption 2

```
cMe=s(1) !Maleic acid

cMi=s(2) !Malic acid

cMo=s(3) !Malonic acid

cSA=s(4) !Succinic acid

cHP=s(5)!H2O2

cFoA=s(6) !Formic acid

cFumA=s(7) !Fumaric acid

cHf=s(8) !2(5)H furanone

cFurA=s(9) !Furoic acid

cF=s(10) !Furfural

cCO2=s(11) ! CO2 in gas phase


Temp=Tempc+273.15d0

Tmean=Tmeanc+273.15d0


z=1.0d0/Temp-1.0d0/Tmean

k1=km1*exp(-E1/8.3143d0*z)

k2=km2*exp(-E2/8.3143d0*z)

k3=km3*exp(-E3/8.3143d0*z)
```

```
k4=km4*exp(-E4/8.3143d0*z)

k5=km5*exp(-E5/8.3143d0*z)

k6=km6*exp(-E6/8.3143d0*z)

k7=km7*exp(-E7/8.3143d0*z)

k8=km8*exp(-E8/8.3143d0*z)

k9=km9*exp(-E9/8.3143d0*z)

k9r=km9r*exp(-E9r/8.3143d0*z)


vr=403.245d0

vg=vr-vl

rhoc=mcat/vl

alpha=vl/vg


rFurA=k1*cF*cHP*rhoc

rSA=k6*cF*cHP

rHf=k3*cF*cHP

rMe=k8*cF*cHP+k9*cFumA-k9r*cMe

rFumA=cF*cHP*k7+k9r*cMe-k9*cFumA

rMi=cF*cHP*k5

rCO2=k4*cFoA*cHP

rFoA=k2*cF+rFurA +rMi+rSA+cF*cHP*(k7+k8)-rCO2

rF=-rFurA-rHf-k2*cF-rMi-rSA-cF*cHP*(k7+k8)

rHP=-rco2-rFurA-rSA-rMi-(k8+k7)*cFoA*cHP-rHf


ds(1)=rMe

ds(2)=rMi
```

ds(3)=0.0d0

ds(4)=rSA

ds(5)=rHP

ds(6)=rFoA

ds(7)=rFumA

ds(8)=rHf

ds(9)=rFurA

ds(10)=rF

ds(11)=(rCO2*alpha-cCO2*vout/vg)/((alpha/ki)+1)

Appendix II

Table A-1 Molecular Masses of Compounds Considered in the Present Thesis [28]

Name	Molecular mass [g/mol]
2 (5H) furanone	84.10
Carbon dioxide	44.00
Formic acid	46.03
Fumaric acid	116.07
Furfural	96.084
Furoic acid	112.08
Hydrogen peroxide	34.01
Maleic acid	116.07
Malic acid	134.09
Malonic acid	104.06
Succinic acid	118.09
Water	18.01

References

[1] W. Reutemann and H. Kieczka, “Furfural,” *Ullmann’s Encycl. Ind. Chem.*, vol. D, 285–313, 2012.

[2] G. Goor, J. Glenneberg, and S. Jacobi, “Hydrogen Peroxide,” *Ullmann’s Encycl. Ind. Chem.*, 394–427, 2000.

[3] “Succinic Acid.” [Online]. Available: https://www.thechemco.com/chemical/succinic-acid/. [Accessed: 25-May-2016].

[4] T. Werpy and G. Petersen, “Top Value Added Chemicals from Biomass Volume I — Results of Screening for Potential Candidates from Sugars and Synthesis Gas Top Value Added Chemicals From Biomass Volume I : Results of Screening for Potential Candidates,” 2004.

[5] “BioAmber is a Sustainable Chemicals Company Offering Choice, Naturally.” [Online]. Available: https://www.bio-amber.com/bioamber/en. [Accessed: 25-May-2016].

[6] “Bio-succinic acid.” [Online]. Available: http://www.myriant.com/products/bio-succinic-acid.cfm. [Accessed: 27-May-2016].

[7] E. J. Molga and K. R. Westerterp, “Principles of chemical reaction engineering,” *Ullmann’s Encyclopedia of Industrial Chemistry*. 1–99, 2013.

[8] T. Salmi, J.-P. Mikkola, and J. Wärnå, *Chemical reaction engineering and reactor technology*. Turku: Boca Raton, Fla. : CRC, 2011., 2011.

[9] O. Levenspiel, *Chemical reaction engineering*. New York : Wiley, 1972.

[10] K. J. Laidler, *Chemical kinetics*. New York : McGraw-Hill, 1987.

[11] M. G. Evans and M. Polanyi, “Inertia and driving force of chemical reactions,” *Trans. Faraday Soc.*, 34, 11–24, 1938.

[12] U. Mann, “Reactor Technology,” in *Kirk-Othmer Encyclopedia of Chemical Technology*, John Wiley & Sons, Inc., 2006.

[13] J. Schlauer, “Absorption, 1. Fundamentals,” in *Ullmann’s Encyclopedia of Industrial Chemistry*, Wiley-VCH Verlag GmbH & Co. KGaA, 2000.

[14] N. Musakka, T. Salmi, J. Wärnå, and J. Ahlkvist, “Modelling of liquid-phase decomposition reactions through gas-phase product analysis : model systems and peracetic acid,” *Chem. Eng. Sci.*, 61, 6918–6928, 2006.

[15] H. Harrio, “User’s guide.pdf.” ProfMath Oy, Helsinki, 2001.

[16] S. C. McCutcheon and B. Martin, J.L, “Water Quality,” in *Handbok of Hydrology*, D. R. Maidment, Ed. New York : McGraw Hill, 1993, p. 11.3.

[17] Aldrich Chemical Company Inc., “2(5H)-Furanone,” in *Catalog Handbook of Fine Chemicals*, Milwaukee WI: National Institute of Standards and Technology, 1990.

[18] J. Hietala, A. Vuori, P. Johnsson, I. Pollari, W. Reutemann, and H. Kieczka, “Formic Acid,” in *Ullmann’s Encyclopedia of Industrial Chemistry*, Helsinki: Wiley-VCH Verlag GmbH & Co. KGaA, 2000, 1–22.

[19] “malic acid | C4H6O5 - PubChem.” [Online]. Available: https://pubchem.ncbi.nlm.nih.gov/compound/525#section=Odor. [Accessed: 27-May-2016].

[20] D. W. Green and R. H. Perry, “Vapor Pressures of Pure Substances,” *Perry’s Chemical Engineers' Handbook, Eighth Edition*. McGraw Hill Professional, Access Engineering, New York, 2008.

[21] J. J. Carroll and A. E. Mather, “The solubility of hydrogen sulphide in water from 0 to 90°C and pressures to 1 MPa,” *Geochim. Cosmochim. Acta*, 53, 1163–1170, 1989.

[22] J. J. Caroll, J. D. Slupsky, and A. E. Mather, “The solubility of Carbon Dioxide in Water at Low Pressure,” *J.Phys.Chem.Ref.Data*, 20, 6, 1–26, 1991.

[23] J. J. Carroll and A. E. Mather, “The system carbon dioxide-water and the Krichevsky-Kasarnovsky equation,” *J. Solution Chem.*, 21, 7, 607–621, 1992.

[24] N. N. Akinfiev and L. W. Diamond, “Thermodynamic description of aqueous nonelectrolytes at infinite dilution over a wide range of state parameters,” 67, 4, 613–627, 2003.

[25] R. M. Enick, G. D. Holder, and R. Mohamed, “Four-Phase Flash Equilibrium Calculations Using the Peng-Robinson Equation of State and a Mixing Rule for Asymmetric Systems,” *Soc. Pet. Eng.*, 2, 04, 687 – 694, 1987.

[26] M. J. McFarland, “Solubility of Gases in Water,” *Biosolids Engineering*. McGraw Hill Professional, Access Engineering, New York, 2001.

[27] P. G. T. Fogg and W. Gerrard, *Solubility of gases in liquids : a critical evaluation of gas/liquid systems in theory and practice*. Chichester : Wiley, 1991.

[28] “Home - PubChem Compound - NCBI.” [Online]. Available: https://www.ncbi.nlm.nih.gov/pccompound. [Accessed: 25-May-2016].